Estimation of Muscle Fiber Conduction Velocity from Simulated Surface EMG in Pinnate Muscles

Terms of use:

Publisher copyright

(Article begins on next page)

15 May 2024

Estimation of Average Muscle Fiber Conduction Velocity

from Simulated Surface EMG in Pinnate Muscles

Luca Mesin[1], Luisa Damiano[1], Dario Farina[2,*]

[1]Laboratorio di Ingegneria del Sistema Neuromuscolare (LISiN), Dipartimento di Elettronica, Politecnico di Torino, Torino, Italy
[2] Center for Sensory-Motor Interaction (SMI), Department of Health Science and Technology
Aalborg University, Aalborg, Denmark

Address for correspondence
* Dario Farina, Ph.D.
Center for Sensory-Motor Interaction
Aalborg University
Fredrik Bajers Vej 7 D-3, DK-9220 Aalborg, Denmark
tel: +4596358821; fax: +4598154008
E-mail: df@hst.aau.dk

ABSTRACT

The aim of this simulation study was to assess the bias in estimating muscle fiber conduction velocity (CV) from surface electromyographic (EMG) signals in muscles with one and two pinnation angles. The volume conductor was a layered medium simulating anisotropic muscle tissue and isotropic homogeneous subcutaneous tissue. The muscle tissue was homogeneous for one pinnation angle and inhomogeneous for bipinnate muscles (two fiber directions). Interference EMG signals were obtained by simulating recruitment thresholds and discharge patterns of a set of 100 and 200 motor units for the pinnate and bipinnate muscle, respectively (15° pinnation in both cases). Without subcutaneous layer and muscle fibers with CV 4 m/s, average CV estimates from the pinnate (bipinnate) muscle were 4.81 ± 0.18 m/s (4.80 ± 0.18 m/s) for bipolar, 4.71 ± 0.19 m/s (4.71 ± 0.12 m/s) for double differential, and 4.78 ± 0.16 m/s (4.79 ± 0.15 m/s) for Laplacian recordings. When subcutaneous layer was added (thickness 1 mm) in the same conditions, estimated CV values were 4.93 ± 0.25 m/s (5.16 ± 0.41 m/s), 4.70 ± 0.21 m/s (4.83 ± 0.33 m/s), and 4.89 ± 0.21 m/s (4.99 ± 0.39 m/s), for the three recording systems, respectively. The main factor biasing CV estimates was the propagation of action potentials in the two directions which influenced the recording due to the scatter of the projection of end-plate and tendon locations along the fiber direction, as a consequence of pinnation. The same problem arises in muscles with the line of innervation zone locations not perpendicular to fiber direction. These results indicate an important limitation in reliability of CV estimates from the interference EMG when the innervation zone and tendon locations are not distributed perpendicular to fiber direction.

1. INTRODUCTION

Surface electromyographic (EMG) signals may be used for the estimation of muscle fiber conduction velocity (CV) (Arendt-Nielsen & Zwarts, 1989). For this purpose, two or more detection systems are placed along the direction of muscle fibers. Under the hypothesis of space-invariant volume conductors (Farina et al., 2004b), the properties of the tissues interposed between the signal sources and the detection electrodes do not vary along the muscle fiber direction, thus, for infinite fibers, the potentials detected at the skin surface in any location along the fiber direction have the same shape. However, in the experimental case, volume conductors are inhomogeneous. Furthermore, the generation of the action potential at the end-plate and the extinction at the tendons introduce non-travelling signal components (Arabadzhiev et al., 2003; 2004). When the signals detected at different locations along fiber direction do not have the same shape, the definition of propagation delay is not unique (Farina & Merletti, 2004).

Inhomogeneities in the volume conductor may be due to local (Mesin & Farina, 2005) or distributed (Mesin & Farina, 2006) changes in conductivity. Muscles with more than one fiber orientation are also inhomogeneous since the conductivity of the muscle tissue depends on fiber orientation. Thus, bipinnate muscles constitute non-space invariant volume conductors (Mesin & Farina, 2004). Simulation of EMG signals generated by these muscles indeed revealed variability of the surface detected fiber action potentials along the direction of propagation (Mesin & Farina, 2004). Another important feature of muscle fibers located at a certain pinnation angle is that the projection of end-plate and tendon locations on the direction of the fibers may have large scatter, which depends on the pinnation angle. Thus, a set of surface EMG systems placed in the direction of the muscle fibers detects potentials propagating in opposite directions or non-propagating (Figure 1). A similar effect occurs in muscles with fibers perpendicular to the line of action but end-plate location along a line not perpendicular to fiber direction, such as the upper trapezius muscle (Farina et al., 2006). The bias introduced by the propagating of action potentials in the opposite direction with respect to the semi-fiber length where the detection systems are placed was recognized also in

case of parallel fibers and innervation zone perpendicular to them (Dimitrov & Dimitrova, 1974; Gydikov et al., 1976).

The aim of the study was to investigate factors affecting CV estimates from simulated EMG signals generated by muscles with one and two pinnation angles.

Figure 1 about here

2. METHODS

2.1 Volume conductor

Two volume conductor models were used. The first consisted of fibers with only one pinnation angle, the second of fibers with two pinnation angles. The other parameters were the same for the two models. The inclusion of a bundle of fibers with different pinnation angle with respect to that over which the electrodes are located makes the volume conductor inhomogeneous in the direction of source propagation (Mesin & Farina, 2004). Thus, the action potentials change shape during propagation even in the absence of generation and extinction at the end-plate and tendons. The use of the two models allowed us to investigate if the presence of more than one pinnation angle was the main factor affecting CV estimates in pinnate muscles.

2.1.1 Muscle with one pinnation angle

The analytical model used to simulate muscles with a single pinnation angle describes the volume conductor as a two-layer medium, with isotropic subcutaneous tissue (conductivity $\sigma = 0.05$ S/m) and anisotropic muscle tissue (transversal and longitudinal conductivities $\sigma_T = 0.1$ S/m and $\sigma_L = 0.5$ S/m, respectively). The method proposed in (Farina & Merletti, 2001) was applied to calculate the analytical transfer function of the two-layer volume conductor, from which the impulse response was evaluated by numerical inversion of the two-dimensional Fourier transform. The subcutaneous layer was infinite in the x and z directions and 1 mm thick, bounded on one side by air (modeled as a non-conductive medium) and on the other side by the muscle

4

tissue. The muscle layer was semi-infinite in the *y* direction and infinite in the *x* and *z* directions. Tendons were located in order to simulate a muscle with pinnation angle 15° (Figure 2A). Fiber end-plates were in the middle of the muscle fibers.

2.1.2 Muscle with two pinnation angles

For bipinnate muscle, the muscle tissue was modeled as an inhomogeneous, anisotropic medium, semi-infinite in the *y* direction, infinite in the *x* and *z* directions. Transversal and longitudinal conductivities were the same as for the case of one pinnation angle. The impulse response for this volume conductor was derived in (Mesin & Farina, 2004). A planar subcutaneous layer, 1 mm thick ($\sigma = 0.05\,\mathrm{S/m}$), was added to the volume conductor, as described in (Mesin, 2005). An approximate analytical expression for the impulse response was obtained as described in (Mesin, 2005). The two models of volume conductor were thus identical with the only difference of the conductivity tensor which was influenced by the second bundle of fibers in the bipinnate muscle.

Figure 2 about here

2.2 Sources and detection systems

For both volume conductor models, the intracellular action potentials originated at the end-plate, propagated along the fibers, and extinguished at the tendons. The transmembrane current density (second derivative of the intracellular action potential) was modeled as a current tripole with impulse amplitudes I_1 = 24.6 A/m^2, I_2 = -35.4 A/m^2, and I_3 = 10.8 A/m^2, and distances between impulses a = 2.1 mm and b = 4.8 mm (Figure 2a) (McGill & Huynh, 1988; Merletti et al., 1999). The signal was detected with monopolar, single differential (SD), double differential (DD), and Normal Double Differential (NDD) systems (Disselhorst-Klug et al., 1997). In all cases, a 3×8

electrode grid was simulated (Figure 3) which led, for the central column, to 8 monopolar, 7 SD, and 6 DD and NDD detected signals.

2.3 Numerical implementation

The analytical solution for the impulse response of the bipinnate muscle volume conductor was obtained in the two-dimensional Fourier domain (angular frequencies k_x, k_z in the x and z directions, respectively), for a set of planes along the y variable (Figure 2B). k_x and k_z were sampled over 256 points with maximum values corresponding to a sampling frequency in time domain of 4096 Hz for CV 4 m/s [see (Farina & Merletti, 2001) for the relation between spatial and temporal frequencies].

Since the model is not space invariant (Farina et al., 2004a), impulse responses were simulated for sampled positions of the sources. The simulated positions (x_s, y_s, z_s) of the impulses in the source tripole were $x_s = 0$; $y_s = 2, 3.5, 5$ mm within the muscle; and z_s (distance from the pinnation line) in the range 1-30 mm (0.5 mm increment). The same locations of the sources over time were used in case of pinnate muscle. Intermediate depths within the muscle were treated by averaging the impulse responses corresponding to the two closest depths (Figure 2B). The impulse responses in different positions along the x direction were simulated by translating the simulated impulse responses (since in the x direction the volume conductor is invariant). The impulse responses in different positions along the z direction were obtained by a linear (convex) combination of the impulse responses placed at the closest sampling points of the z variable. Five depths within the muscle were simulated by a linear (convex) combination of the impulse responses placed at the closest sampling points of the y variable.

Transversal distances from the detection array were simulated by shifting the matrix (which is equivalent to shifting the fiber) in the positive and negative x direction, with 20 sampling steps

and maximum translation of 30 mm in both directions. The location of the fibers within the volume conductor was thus limited to 30-mm transversal distance and 5-mm depth to reduce the computation load. Although more distant fibers may contribute to the interference signal, their effect on estimates of average conduction velocity is limited due to attenuation of their action potentials by the tissues interposed.

From all impulse responses for the infinite bipinnate muscle, the homogeneous Dirichlet and Neumann problem was solved applying the image theorem (Mesin, 2005), and the subcutaneous layer was added over the muscle as described in (Mesin, 2005).

2.4 Motor unit action potentials

One-hundred motor units for each fiber bundle were simulated, i.e., 100 for the pinnate and 200 for the bipinnate muscle in total. Motor unit CV distribution (Gaussian) had mean 4 m/s while standard deviation was fixed to 0 m/s (all motor units with 4 m/s CV) and 0.5 m/s in two simulation sets. The number of fibers in each motor unit varied randomly in the range 50-800. To reduce computational time, all fibers in each motor unit were concentrated along a line, with spread of the end-plates 10 mm (adding delayed versions of one simulated single fiber action potential). End-plates were located on average in the middle of the fiber length. Fiber length was 75 mm in all cases.

2.5 Discharge patterns

Motor units were recruited according to the following recruitment threshold excitation (RTE) function (Fuglevand et al., 1993):

$$RTE(i) = e^{\ln(RR)i/n} \quad i = 1, 2, ..., n \tag{2}$$

where i is an index identifying the motor neurons, RR is the range of recruitment thresholds (100% in this study), and n is the total number of motor units in the simulated pool.

The discharge statistics were modeled assuming minimum and maximum discharge rates of 8 and 35 pulses per second (pps), linear relation between force and discharge rate (0.5 pps/%MVC for all MUs), and Gaussian distribution of the interpulse interval variability (coefficient of variation 0.2). The excitation level simulated was 100% in all cases. In case of a distribution of CV with non-zero standard deviation, the motor units were recruited from low to high conduction velocities (Andreassen & Arendt-Nielsen, 1987). Simulated signals were 10-s long.

2.6 Signal analysis

CV was estimated from each pair of consecutive simulated EMG derivations (7 pairs for the monopolar recordings, six for the single differential, and five for both the double differential and normal double differential) with the spectral matching approach (McGill & Dorfman, 1984). The spectral matching approach is theoretically equivalent to the crosscorrelation method (Merletti & Lo Conte, 1995) and is one of the most commonly applied techniques for estimation of conduction velocity from surface EMG. The estimator resulting from the spectral matching corresponds to the maximum likelihood estimator (minimum variance) in case of white Gaussian noise (Farina & Merletti, 2004). Ten CV estimates were obtained dividing each 10-s long simulated signal into epochs of 1 s. The 10 estimates were averaged to obtain a single representative value for each detection system and each pair of derivations. In each condition, 10 simulations were performed, randomly varying the distribution of sizes of the motor units within the muscle. Results are thus presented as mean values and standard deviations across the 10 simulations in each condition.

RESULTS

Figure 4 shows representative single fiber action potentials, detected by seven bipolar recordings. The transversal displacement of the fiber in the left and right direction with respect to the detection system (Figure 4B,C) corresponds to decreased amplitude and increased duration of the propagating component, due to the low-pass filtering effect of the volume conductor. The

direction of propagation of the simulated action potentials detected by the array in line with the muscle fibers depends on the distance of the fiber from the detection systems. This is due to the large scatter in the projection of end-plate and tendon locations along the fiber direction. When comparing single fiber action potentials generated by pinnate and bipinnate muscles, the differences in shape were rather small and due to different conductivity tensors of the two volume conductors (Mesin & Farina, 2004). In the case of bipinnate muscle, however, a second set of fibers is active, producing non-propagating action potentials (Figure 4D) in the interference EMG signal recorded over the other bundle.

Figure 4 about here

Figure 5 shows an example of monopolar interference signals. The bias in CV estimates was positive for the four models considered (pinnate/bipinnate, with or without subcutaneous layer) (Figure 6). It was larger for monopolar recordings with respect to the others and for locations closer to the tendon. Moreover, bias increased when subcutaneous layer was included in the volume conductor. When a distribution of CV was simulated, bias increased due to the larger weight of the larger motor units with higher CV on the average CV estimates (Table I).

Figures 5 and 6 and Table 1 about here

DISCUSSION

This paper addressed the problem of estimating CV from surface EMG signals recorded from pinnate muscles. With respect to muscles with straight fibers, the signals detected from pinnate muscles along the fiber direction are affected by a variable location of the projection of end-

plates and tendons along the array of electrodes. This introduces problems in the estimation of CV from the interference EMG signal.

The results showed that even in case of single pinnation angle, CV estimates presented large bias that increased when subcutaneous layer was included in the volume conductor. The difference in CV bias between single and double pinnation angle was very limited without subcutaneous layer, indicating that the second bundle of fibers in the bi-pinnate muscle influenced the characteristics of the signal in a negligible way. This is due to the relative large distance between the second bundle of fibers and the recording electrodes. When subcutaneous layer was added, the electrode-source distances were less different for the two bundles and the relative contribution from the second bundle increased. The effect of this factor to the total bias was limited but increased substantially with thicker subcutaneous layers (results not shown). In the simulations shown, the main effect on CV estimates was due to the scattered projection of end-plates and tendons along the recording electrodes resulting from the inclination of the muscle fibers.

In this study the end-plates were located in the middle of the fiber length and the pinnation angle was fixed to 15°. These choices determined a specific location of the projection of the end-plates on the array direction and thus a specific bias in CV. Different choices of location of end-plates and/or pinnation angle would have determined different results. For example, if the innervation zone locations were along a line perpendicular to the array orientation (i.e., to the muscle fibers), the array would have been distal to the projection of the end-plates of all fibers. However, this would imply that the end-plates should be very close to the tendons for some fibers. In addition, even in this condition, the problem of the projection of the tendon region could not be avoided and would lead to similar problems as observed in these simulations. Similarly, for clarity, results on only one pinnation angle, one interelectrode distance and one thickness of the subcutaneous layer are shown. The qualitative effect of varying these parameters can be predicted from the simulations shown and from previous studies (e.g., Arabadzhiev et al., 2003). The main result of this study is the observation that oblique position of innervation zones and tendons with

respect to fiber orientation implies bias in CV estimates. This bias depends on the relative weight of the components propagating in two opposite directions in the interference signal.

The effect of opposite propagation directions on CV estimates has been underlined in previous work that considered parallel fibers with the same average location of the end-plates (Dimitrov & Dimitrova, 1974; Gydikov et al., 1976). The present study indicates that this problem is enhanced in muscles with innervation zones located along a line not perpendicular to fiber orientation even if the fibers are parallel to the line of action (no pinnation angle). Distribution of innervation zones not perpendicular with fiber direction is very common (Masuda et al., 1983). Figure 7, for example, shows this situation in the upper trapezius muscle investigated with two-dimensional EMG recordings. Oblique location of innervation zones with respect to the fiber direction can explain the difficulties in reliably estimating CV even from muscles with parallel and relatively long fibers, e.g., upper trapezius (Sjøgaard et al., 2006) and vastus lateralis (Rainoldi et al., 2001), and the usually larger values of CV estimates obtained from the surface EMG with respect to those obtained from intramuscular EMG (Zwarts, 1989).

Figure 7 about here

The CV bias cannot be predicted a-priori since it depends on anatomical factors that are likely different across subjects. From Table 1, it is noted that the standard deviation of estimation over different simulations is larger for monopolar signals, probably due to a larger weight of non-propagating signal components in this recording modality.

A possible solution to the problem of biased average CV is the identification of single peaks or motor unit action potentials (e.g., Beck et al., 2005a; 2005b; Hogrel, 2003) from the interference EMG and estimation of CV values for each action potential. In this case, it is possible to consider only estimates from motor units close to the detection point for which the recording electrodes are

between the innervation zone and tendon. However, this requires more complex processing algorithms.

In conclusion, estimates of CV using surface EMG from pinnate muscles are affected by positive bias. This explains the large values of average CV often reported in the literature from pinnate muscles or muscles with innervation zones location not perpendicular to the muscle fiber direction and poses limitations to the technique of estimating CV from surface EMG signals.

GRANTS

REFERENCES

Andreassen S, Arendt-Nielsen L. Muscle fiber conduction velocity in motor units of the human anterior tibial muscle: a new size principle parameter. J Physiol. 1987;391:561-71.

Arabadzhiev TI, Dimitrov GV, Dimitrova NA. Simulation analysis of the ability to estimate motor unit propagation velocity non-invasively by different two-channel methods and types of multi-electrodes. J Electromyogr Kinesiol. 2003;13:403-15.

Arabadzhiev TI, Dimitrov GV, Dimitrova NA. The cross-correlation and phase-difference methods are not equivalent under noninvasive estimation of the motor unit propagation velocity. J Electromyogr Kinesiol. 2004;14:295-305.

Arendt-Nielsen L, Zwarts M. Measurement of muscle fiber conduction velocity in humans: techniques and applications. J Clin Neurophysiol. 1989;6:173-90.

Beck RB, O'Malley MJ, Stegeman DF, Houtman CJ, Connolly S, Zwarts MJ. Tracking motor unit action potentials in the tibialis anterior during fatigue. Muscle Nerve. 2005a;32:506-14.

Beck RB, Houtman CJ, O'Malley MJ, Lowery MM, Stegeman DF. A technique to track individual motor unit action potentials in surface EMG by monitoring their conduction velocities and amplitudes. IEEE Trans Biomed Eng. 2005b;52:622-9.

Dimitrov GV, Dimitrova NA. Extracellular potential field of a single striated muscle fibre immersed in anisotropic volume conductor. Electromyogr Clin Neurophysiol. 1974;14:423-36.

Disselhorst-Klug C, Silny J, Rau G. Improvement of spatial resolution in surface-EMG: a theoretical and experimental comparison of different spatial filters. IEEE Trans Biomed Eng. 1997; 44:567–74.

Farina D, Merletti R. A novel approach for precise simulation of the EMG signal detected by surface electrodes. IEEE Trans Biomed Eng. 2001;48:637-46.

Farina D, Merletti R. Methods for estimating muscle fibre CV from surface electromyographic signals. Med Biol Eng Comput. 2004;42:432-45.

Farina D, Mesin L, Martina S. Advances in surface electromyographic signal simulation with analytical and numerical descriptions of the volume conductor. Med Biol Eng Comput. 2004a;42:467-76.

Farina D, Pozzo M, Merlo E, Bottin A, Merletti R. Assessment of muscle fiber conduction velocity from surface EMG signals during fatiguing dynamic contractions. IEEE Trans Biomed Eng. 2004b;51:1383-93.

Farina D, Leclerc F, Arendt-Nielsen L, Battelli O, Madeleine P. The change in spatial distribution of upper trapezius muscle activity is correlated to contraction duration. J Electromyogr Kinesiol. Submitted.

Fuglevand AJ, Winter DA, Patla AE. Models of recruitment and rate coding organization in motor-unit pools. J Neurophysiol. 1993;70:2470-88.

Gydikov A, Gerilovsky L, Dimitrov GV. Volume conducted motor unit potentials in human triceps surae. Electromyogr Clin Neurophysiol. 1976;16:569-86.

Hogrel JY. Use of surface EMG for studying motor unit recruitment during isometric linear force ramp. J Electromyogr Kinesiol. 2003;13:417-23.

Jensen C, Vasseljen O, Westgaard RH. The influence of electrode position on bipolar surface electromyogram recordings of the upper trapezius muscle. Eur J Appl Physiol Occup Physiol. 1993;67:266-73.

Masuda T, Miyano H, Sadoyama T. The distribution of myoneural junctions in the biceps brachii investigated by surface electromyography. Electroencephalogr Clin Neurophysiol. 1983;56:597-603.

McGill KC, Dorfman LJ. High-resolution alignment of sampled waveforms. IEEE Trans Biomed Eng. 1984;31:462-8.

McGill K, Huynh A. A model of the surface recorded motor unit action potential. Proc 10th Ann Int IEEE Conf Eng Med Biol. 1988;1697-9.

Merletti R, Lo Conte LR. Advances in processing of surface myoelectric signals: Part 1. Med Biol Eng Comput. 1995;33:362-72.

Merletti R, Lo Conte L, Avignone E, Guglielminotti P. Modelling of surface myoelectric signals – part I: model implementation. IEEE Trans Biomed Eng. 1999;46:810-20.

Mesin L, Farina D. Simulation of surface EMG signals generated by muscle tissues with in-homogeneity due to fiber pinnation. IEEE Trans Biomed Eng. 2004;51:1521-9.

Mesin L, Farina D. A model for surface EMG generation in volume conductors with spherical inhomogeneities. IEEE Trans Biomed Eng. 2005;52:1984-93.

Mesin L, Farina D. An analytical model for surface EMG generation in volume conductors with smooth conductivity variations. IEEE Trans Biomed Eng. In press (2006).

Mesin L. Analytical generation model of surface electromyogram for multi layer volume conductors. In: Modelling in Medicine and Biology VI, WIT Transactions on Biomedicine and Health (ISSN 1743-3525), 2005:95-110.

Rainoldi A, Bullock-Saxton JE, Cavarretta F, Hogan N. Repeatability of maximal voluntary force and of surface EMG variables during voluntary isometric contraction of quadriceps muscles in healthy subjects. J Electromyogr Kinesiol. 2001;11:425-38.

Sjogaard G, Sogaard K, Hermens HJ, Sandsjo L, Laubli T, Thorn S, Vollenbroek-Hutten MM, Sell L, Christensen H, Klipstein A, Kadefors R, Merletti R. Neuromuscular assessment in elrderly workers with and without work related shoulder/neck trouble: the NEW-study design and physiological findings. Eur J Appl Physiol. 2006;96:110-21.

Zwarts MJ. Evaluation of the estimation of muscle fiber CV. Surface versus needle method. Electroencephalogr Clin Neurophysiol. 1989;73:544-8.

Table 1 Average (SD) (over all locations along the array) CV estimates in the conditions analyzed.

SD: single differential; DD: double differential; NDD: Laplacian.

FIGURE CAPTIONS

Figure 1 Schematic representation of a bipinnate muscle with a recording array aligned with fiber orientation and located between end-plate and tendon of the underlying fiber. The fibers at transversal distance from the array contribute with action potentials propagating in both directions (projection of the end-plate) or non-propagating (projection of the tendon). The array cannot be located between end-plate and tendon of all fibers in this anatomical condition.

Figure 2 Model of bipinnate and pinnate muscle. A) Definition of pinnation angle and tripole source. (B) The two-layer model consists of subcutaneous layer (1-mm thick in this study) and semi-infinite muscle tissue. Three depths within the muscle were simulated. Two intermediate depths were obtained by linear combinations of the simulated impulse responses.

Figure 3 Schematic representation of the simulated fibers and detection grid. Note the different orientation of the conductivity tensor in the two portions of the volume conductor.

Figure 4 Representative examples of simulated single fiber action potentials, detected by an array of seven bipolar systems. Four fibers at 2 mm depth within the muscle were simulated (A-D). Both pinnate (solid line) and bipinnate (dashed line) muscles were considered with subcutaneous layer 1-mm thick. The different conductivity tensors in the two cases determined small differences between the generated surface action potentials. The potential generated by a fiber belonging to the second fiber bundle of the bipinnate muscle is also shown (D). In B-D the first derivative of the intracellular action potential and its direction of propagation are schematically shown.

Figure 5 Example of monopolar interference signal (A). Two zoomed portions of the interference signal (B) show different propagation paths of the detected potentials.

Figure 6 Estimated CV for the four models considered (pinnate and bipinnate, with and without subcutaneous layer) for monopolar (A), single differential (B), double differential (C), and Laplacian (D) recordings. SD: single differential; DD: double differential; NDD: Laplacian; CV: conduction velocity.

Figure 7 Map of surface EMG root mean square value from experimental recordings from the upper trapezius muscle with a 5×13 electrode grid. The electrode grid (8-mm interelectrode distance in both directions) was placed with the 4th row along the seventh cervical vertebra - acromion line and with the most medial electrode column 10-mm distant from the innervation zone location. The rows of the grid are approximately parallel to the fiber orientation according to Jensen et al. (1993). The subject was standing in erect position with the shoulders 90° abducted without hand load, as described in detail in (Farina et al., 2006). White areas correspond to high values and dark areas to low values of root mean square (range 10-120 μV). The dashed line indicates the line of innervation zones, which is not perpendicular to the orientation of the fibers (parallel to the rows of the grid). Any linear array located along the fiber direction would detect signal components propagating in opposite directions due to a similar effect as that schematically depicted for bipinnate muscles in Figure 1.
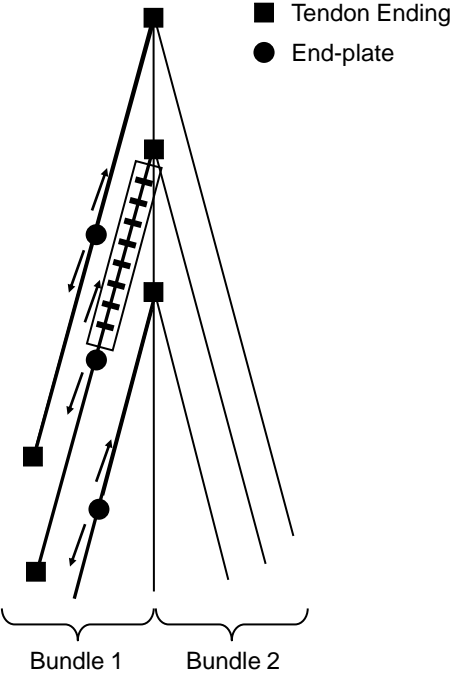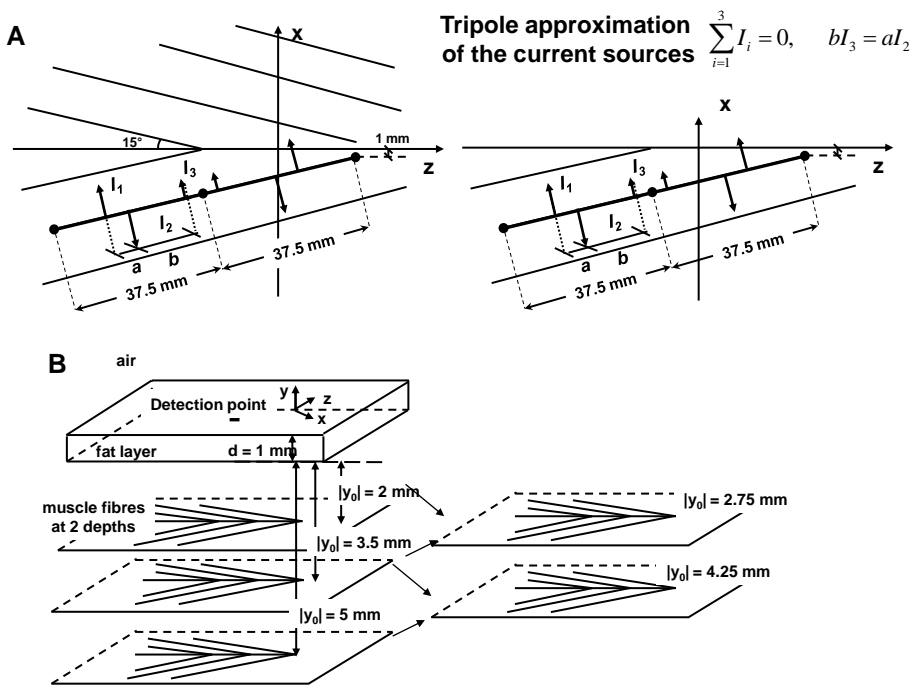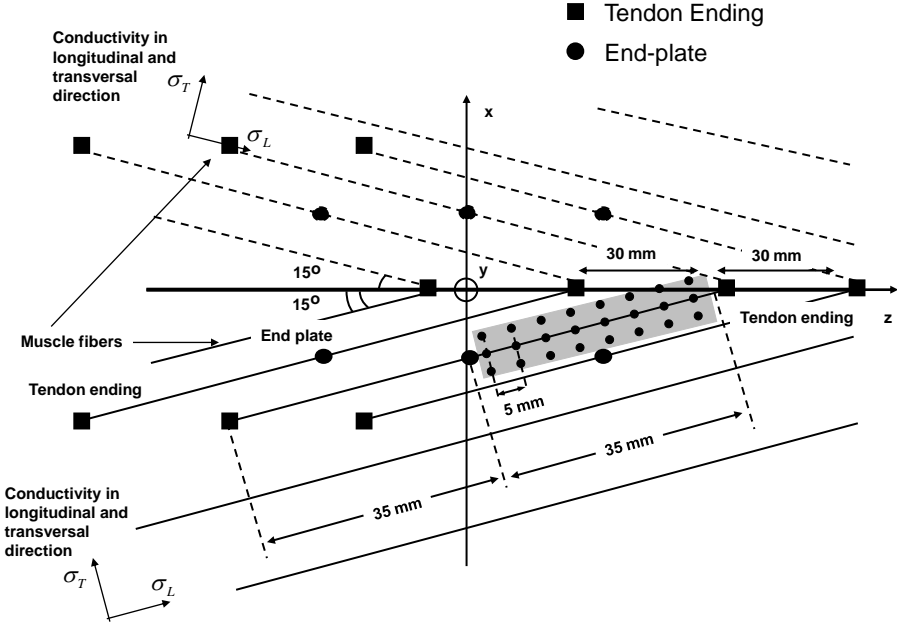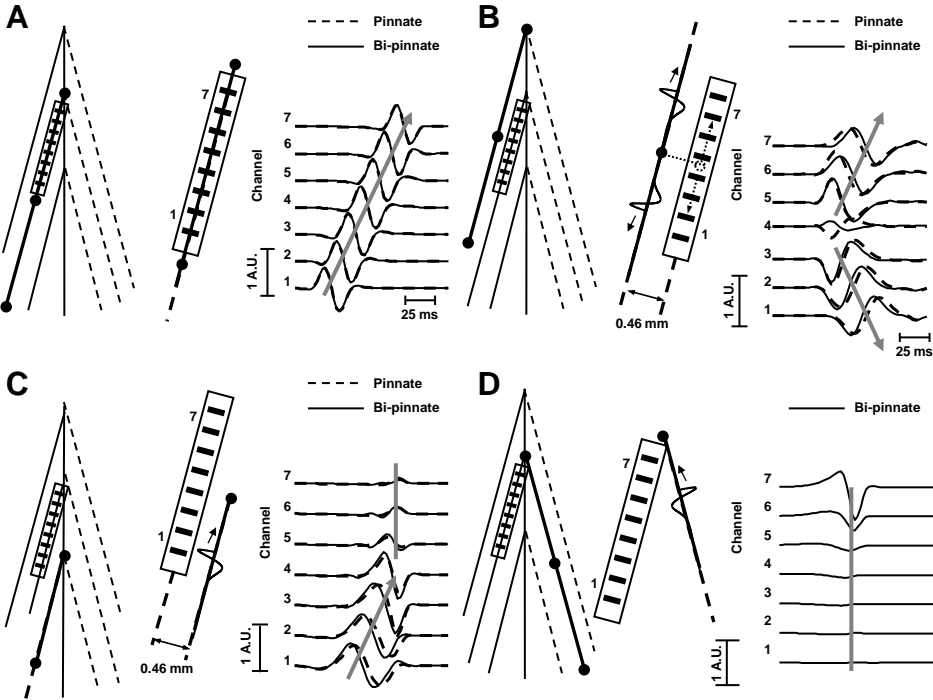
Figure 1

Figure 2

Figure 3

Figure 4

Figure 5

Figure 6

A

Figure 7